Exciton-Trion Polaritons in Doped Two-Dimensional Semiconductors

Farhan Rana,[1] Okan Koksal⬤,[1] Minwoo Jung⬤,[2] Gennady Shvets,[2] A. Nick Vamivakas,[3] and Christina Manolatou[1]

[1]*School of Electrical and Computer Engineering, Cornell University, Ithaca, New York 14853, USA*
[2]*School of Applied and Engineering Physics, Cornell University, Ithaca, New York 14853, USA*
[3]*Institute of Optics, University of Rochester, Rochester, New York, USA*

We present a many-body theory of exciton-trion polaritons (ETPs) in doped two-dimensional semiconductor materials. ETPs are robust coherent hybrid excitations involving excitons, trions, and photons. In ETPs, the 2-body exciton states are coupled to the material ground state via exciton-photon interaction, and the 4-body trion states are coupled to the exciton states via Coulomb interaction. The trion states are not directly optically coupled to the material ground state. The energy-momentum dispersion of ETPs exhibit three bands. We calculate the energy band dispersions and the compositions of ETPs at different doping densities using Green's functions. The energy splittings between the polariton bands, as well as the spectral weights of the polariton bands, depend on the strength of the Coulomb coupling between the excitons and the trions, which in turn depends sensitively on the doping density. The doping density dependence of the ETP bands and the charged nature of the trion states could enable novel electrical and optical control of ETPs.

Very recently, signatures of coherent hybrid excitations involving excitons, trions, and photons in doped two-dimensional (2D) materials have been reported in the literature [1–5]. Although there is no consensus yet on the nature of these hybrid excitations [1–6], these experimental findings are interesting as they call into question the traditional description of a trion as a bound 3-body fermionic state [7–11] consisting of an exciton and a free charge carrier since a fermionic state cannot exist in a coherent superposition with a photon, which is a boson. Several heuristic models describing these polaritons have been proposed in the literature [1–6,12,13]. As discussed in detail in the Supplemental Material [14], these models fall short of describing ETPs accurately, and their shortcomings stem from incomplete descriptions of the exciton and trion states in doped semiconductors.

Several recent works have contributed to clarifying the nature of excitons and trions in doped semiconductors [5,21–25]. Recently, the authors have presented a model based on two coupled Schrödinger equations to describe 2-body excitons and 4-body trions in electron-doped 2D materials [21,22]. A 4-body bound trion state consists of a conduction band electron-hole pair bound to an exciton. The two Schrödinger equations are coupled as a result of Coulomb interactions between the excitons and the trions in doped materials. Good approximate eigenstates of the coupled system can be constructed from superpositions of exciton and trion states. These superpositions include bound and unbound trion states. The latter are exciton-electron scattering states [Fig. 1(a)]. These superposition states resemble the exciton-polaron variational states

proposed by Sidler *et al.* [5,23]. The model developed by the authors [21,22], rather interestingly, also showed that the 4-body trion states have no direct optical matrix elements with the material ground state. The contribution to the material optical conductivity from trion states results almost entirely from the latter's Coulomb coupling to the 2-body exciton states [22] [see Fig. 1(a)].

In this Letter, we present a many-body theory of ETPs in 2D materials [21,22]. The optical coupling between the excitons and the material ground state and the Coulomb coupling between the trions and the excitons result in robust ETPs. The quantum state of ETPs is a coherent superposition of exciton, trion, and photon states. Since the
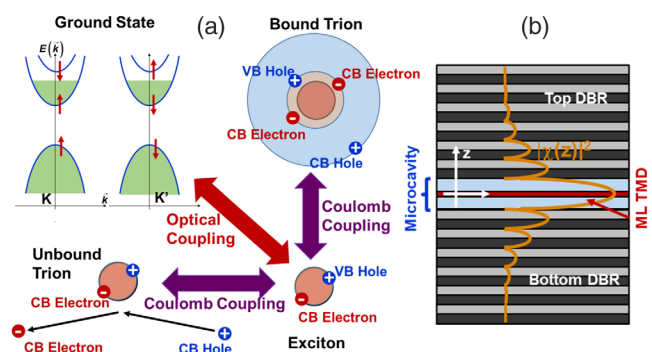

FIG. 1. (a) The nature of couplings among bound and unbound trion states, exciton states, the material ground state, and photons in exciton-trion polaritons (ETPs) is depicted for an electron-doped 2D material (MoSe$_2$) [21,22]. (b) A 2D material monolayer embedded inside an optical microcavity.

4-body trion states also include the continuum of exciton-electron scattering states (or unbound trion states), the polariton problem requires a many-body approach for its complete and accurate description. In the simplest case considered in this work, the ETPs exhibit three bands in their energy-momentum dispersion. The energy splittings between these bands, as well as the spectral weights of these bands, depend on the strength of the Coulomb coupling between the excitons and the trions, which in turn depends on the doping density. Furthermore, exciton-electron scattering, which is inevitable at large electron densities, results in a large broadening of the polariton band closest in energy to the continuum of exciton-electron scattering states (or unbound trion states).

Although the focus in this Letter will be on electron-doped 2D transition metal dichalcogenide (TMD) MoSe$_2$, the arguments are kept general enough to be applicable to other 2D materials. We consider a 2D material monolayer embedded inside an optical microcavity [Fig. 1(b)]. The Hamiltonian describing electrons and holes in the TMD layer (near the K and K' points in the Brillouin zone) interacting with each other and with a transverse-electric-polarized (TE-polarized or in-plane-polarized) cavity optical mode of in-plane momentum $\vec{Q}$ in the rotating wave approximation is [21,22,26–29] as follows:

$$
\begin{aligned}
H = &\sum_{\vec{k},s} E_{c,s}(\vec{k}) c_s^\dagger(\vec{k}) c_s(\vec{k}) + \sum_{\vec{k},s} E_{v,s}(\vec{k}) b_s^\dagger(\vec{k}) b_s(\vec{k}) \\
&+ \frac{1}{A} \sum_{\vec{q},\vec{k},\vec{k}',s,s'} U(q) c_s^\dagger(\vec{k}+\vec{q}) b_{s'}^\dagger(\vec{k}'-\vec{q}) b_{s'}(\vec{k}') c_s(\vec{k}) \\
&+ \frac{1}{2A} \sum_{\vec{q},\vec{k},\vec{k}',s,s'} V(q) c_s^\dagger(\vec{k}+\vec{q}) c_{s'}^\dagger(\vec{k}'-\vec{q}) c_{s'}(\vec{k}') c_s(\vec{k}) \\
&+ \hbar\omega(\vec{Q}) a^\dagger(\vec{Q}) a(\vec{Q}) \\
&+ \frac{1}{\sqrt{A}} \sum_{\vec{k},s} [g_s c_s^\dagger(\vec{k}+\vec{Q}) b_s(\vec{k}) a(\vec{Q}) + \text{H.c.}]
\end{aligned} \tag{1}
$$

Here, $E_{c,s}(\vec{k})$ and $E_{v,s}(\vec{k})$ are the conduction band (CB) and valence band energies. s, s' represent the spin or valley degrees of freedom in the 2D material. $s = \{\sigma, \tau\}$, where $\sigma = \pm 1$ and $\tau = \pm 1$ represent the spin and valley degree of freedom, respectively. m_e (m_h) is the electron (hole) effective mass. $U(\vec{q})$ represents the Coulomb interaction between electrons in the CB and the valence band, and $V(\vec{q})$ represents the Coulomb interaction among the electrons in the CB. $\hbar\omega(\vec{Q})$ is the photon energy, and g_s is the electron-photon coupling constant. g_s is assumed to be nonzero only for the case of the optical coupling between the topmost valence band and the conduction band of the same spin (for $s = \{+1, +1\}$ or $s = \{-1, -1\}$). Other than for phase factors that are not relevant to the discussion in this Letter, the nonzero values of g_s can be written as

[28,29] $g = |g_s| = ev\chi(z=0)\sqrt{\hbar/[2\langle\epsilon\rangle\omega(\vec{Q})]}$, where, v is the interband velocity matrix element [26–29], $\chi(z)$ describes the amplitude of the optical mode in the z direction [Fig. 1(b)], and $\langle\epsilon\rangle$ is the average dielectric constant experienced by the cavity optical mode.

The energy dispersion of ETPs can be found from the poles of the retarded photon Green's function $G^{\text{ph}}(\vec{Q}, t) = -(i/\hbar)\theta(t)\langle[a(\vec{Q}, t), a^\dagger(\vec{Q}, 0)]\rangle$, which satisfies

$$
\begin{aligned}
&\left[\hbar\omega(\vec{Q}) - i\gamma_p + i\hbar\frac{\partial}{\partial t}\right] G^{\text{ph}}(\vec{Q}, t) \\
&= \delta(t) - \frac{\sqrt{2}g}{\sqrt{A}} \sum_{\vec{k}} G_{\vec{Q},T}^{\text{ex-ph}}(\vec{k}; t).
\end{aligned} \tag{2}
$$

Here, $2\gamma_p$ is the inverse photon lifetime in the optical cavity, and

$$
G_{\vec{Q},T}^{\text{ex-ph}}(\vec{k}; t) = -\frac{i}{\hbar}\theta(t)\langle[P_{\vec{Q},T}^\dagger(\vec{k}; t), a^\dagger(\vec{Q}, 0)]\rangle. \tag{3}
$$

$P_{\vec{Q},T}(\vec{k}; t)$ is the transverse polarization operator. In 2D TMDs, one can form superpositions of exciton states from both valleys that couple selectively to either TE-polarized or transverse-magnetic-polarized optical modes [28,29]. For transverse excitons, which couple only to TE-polarized modes, $P_{\vec{Q},T}(\vec{k}; t)$ equals

$$
P_{\vec{Q},T}(\vec{k}; t) = \frac{1}{\sqrt{2}} \sum_s \frac{g_s}{g} c_s^\dagger(\vec{k}+\vec{Q}, t) b_s(\vec{k}, t). \tag{4}
$$

The polarization operator can be obtained from the coupled exciton and trion equations given by Rana et al. [21,22]. Assuming, for simplicity, that the optical mode is coupled to only the nth exciton state in each valley (typically the $n = 0$ state, the lowest energy exciton state, is of interest), the result for the photon Green's function is found to be

$$
[G^{\text{ph}}(\vec{Q}, \omega)]^{-1} = \hbar\omega - \hbar\omega(\vec{Q}) + i\gamma_p - \Sigma^{\text{ph}}(\vec{Q}, \omega), \tag{5}
$$

where the photon self-energy $\Sigma^{\text{ph}}(\vec{Q}, \omega)$ is

$$
\begin{aligned}
\Sigma^{\text{ph}}(\vec{Q}, \omega) = &\sum_s \mathcal{G}_{n,s}^{\text{ex}}(\vec{Q}, \omega) \\
&\times \left| g_s \int \frac{d^2\vec{k}}{(2\pi)^2} \phi_{n,\vec{Q}}^{\text{ex}}(\vec{k}+\lambda_h\vec{Q}) \sqrt{1 - f_{c,s}(\vec{k}+\vec{Q})} \right|^2.
\end{aligned} \tag{6}
$$

Here, $\phi_{n,\vec{Q}}^{\text{ex}}(\vec{k}+\lambda_h\vec{Q})$ is the eigenfunction of the nth exciton state [21,22]. $\lambda_h = 1 - \lambda_e = m_h/m_{\text{ex}}$, $m_{\text{ex}} = m_e + m_h$, and $f_{c,s}(\vec{k})$ are the occupation probabilities for the CB electron states. The bare exciton Green's function $\mathcal{G}_{n,s}^{\text{ex}}(\vec{Q}, \omega)$ (which does not include the contribution to the exciton

self-energy from the exciton-photon interaction) appearing in Eq. (6) is

$$[\mathscr{G}_{n,s}^{\mathrm{ex}}(\vec{Q},\omega)]^{-1} = \hbar\omega - E_{n,s}^{\mathrm{ex}}(\vec{Q}) + i\gamma_{\mathrm{ex}} - \Sigma_{n,s}^{\mathrm{ex}}(\vec{Q},\omega)|_{\mathrm{tr}}. \tag{7}$$

In the above expression, $E_{n,s}^{\mathrm{ex}}(\vec{Q})$ is the energy of the nth exciton state of the spin or valley s [21,22], and γ_{ex} describes the rate of coherence decay of the exciton polarization due to all processes other than exciton-electron scattering. The latter is included explicitly in the exciton self-energy $\Sigma_{n,s}^{\mathrm{ex}}(\vec{Q},\omega)|_{\mathrm{tr}}$ [21,22]. The exciton-electron interaction can be described in terms of exciton-trion coupling [21,22], including couplings to bound and unbound 4-body trion states. The following expression for the exciton self-energy was derived by Rana *et al.* [21]:

$$\Sigma_{n,s}^{\mathrm{ex}}(\vec{Q},\omega)|_{\mathrm{tr}} = \sum_{m,s'}\Sigma_{n,m,s,s'}^{\mathrm{ex}}(\vec{Q},\omega)|_{\mathrm{tr}}$$
$$= \sum_{m,s'}\frac{(1+\delta_{s,s'})|M_{n,m,s,s'}(\vec{Q})|^2}{\hbar\omega - E_{n,m,s,s'}^{\mathrm{tr}}(\vec{Q}) + i\gamma_{\mathrm{tr}}}. \tag{8}$$

The expressions for the Coulomb matrix elements $M_{n,m,s,s'}(\vec{Q})$, coupling 2-body exciton states with spin or valley s to 4-body trion states with spin or valley s, s', can be found in a previous paper by Rana *et al.* [21]. The summation over m above implies a summation over all bound and unbound 4-body trion states consistent with the values of s and s'. $E_{n,m,s,s'}^{\mathrm{tr}}(\vec{Q})$ is the energy of a 4-body trion state and γ_{tr} is a phenomenological parameter describing the decay of the coherence of 4-body correlations. $\Sigma_{n,s}^{\mathrm{ex}}(\vec{Q},\omega)|_{\mathrm{tr}}$ is an increasing function of the doping density [21]. The photon self-energy in Eq. (6) can be written in terms of the optical conductivity of the 2D material [21,22],

$$\Sigma^{\mathrm{ph}}(\vec{Q},\omega) = -i\hbar\frac{|\chi(z=0)|^2}{2\langle\epsilon\rangle}\sigma(\vec{Q},\omega). \tag{9}$$

The dispersion of ETPs can be obtained from the poles of the photon Green's function.

Hopfield coefficients [30,31] play an important role in describing the composition of polariton states. In the case of ETPs, the same information is provided by the spectral density functions, which we discuss next. The photon spectral density function $S^{\mathrm{ph}}(\vec{Q},\omega) = -2\hbar\mathrm{Im}\{G^{\mathrm{ph}}(\vec{Q},\omega)\}$. The spectral density $S_{n,T}^{\mathrm{ex}}(\vec{Q},\omega)$ of the transverse exciton equals $-2\hbar\mathrm{Im}\{G_{n,T}^{\mathrm{ex}}(\vec{Q},\omega)\}$. Assuming $E_{n,s}^{\mathrm{ex}}(\vec{Q}) = E_{n,-s}^{\mathrm{ex}}(\vec{Q})$ and $|g_s| = |g_{-s}|$, the transverse exciton Green's function $G_{n,T}^{\mathrm{ex}}(\vec{Q},\omega)$ is found to be

$$[G_{n,T}^{\mathrm{ex}}(\vec{Q},\omega)]^{-1} = \hbar\omega - E_{n,s}^{\mathrm{ex}}(\vec{Q}) + i\gamma_{\mathrm{ex}} - \Sigma_{n,s}^{\mathrm{ex}}(\vec{Q},\omega)|_{\mathrm{tr}}$$
$$- \Sigma_{n,T}^{\mathrm{ex}}(\vec{Q},\omega)|_{\mathrm{ph}} \tag{10}$$

The spin or valley index s on the right-hand side stands for any one of the two values for which $|g_s| \neq 0$, and the exciton-photon interaction contribution to the transverse exciton self-energy is

$$\Sigma_{n,T}^{\mathrm{ex}}(\vec{Q},\omega)|_{\mathrm{ph}}$$
$$= \sum_s\frac{\left|g_s\int\frac{d^2\vec{k}}{(2\pi)^2}\phi_{n,\vec{Q}}^{\mathrm{ex}}(\vec{k}+\lambda_h\vec{Q})\sqrt{1-f_{c,s}(\vec{k}+\vec{Q})}\right|^2}{\hbar\omega - \hbar\omega(\vec{Q}) + i\gamma_p}. \tag{11}$$

We now assume that only a single bound 4-body singlet trion state of index m exists ($m = 0$ implies the lowest energy bound trion state), and it exists only when the exciton and the bound CB electron-hole pair belong to different valleys (as is the case in MoSe$_2$) [21]. We define a 4-body bound transverse trion state as the one formed by the binding of a CB electron-hole pair to a transverse exciton [21]. Finally, the spectral density function for the bound transverse trion state is $S_{n,m,T}^{\mathrm{tr}}(\vec{Q},\omega) = -2\hbar\mathrm{Im}\{G_{n,m,T}^{\mathrm{tr}}(\vec{Q},\omega)\}$, where the Green's function of the 4-body bound transverse trion state is

$$[G_{n,m,T}^{\mathrm{tr}}(\vec{Q},\omega)]^{-1} = \hbar\omega - E_{n,m,s,-s}^{\mathrm{tr}}(\vec{Q}) + i\gamma_{\mathrm{tr}} - \Sigma_{n,m,T}^{\mathrm{tr}}(\vec{Q},\omega). \tag{12}$$

Here,

$$\Sigma_{n,m,T}^{\mathrm{tr}}(\vec{Q},\omega) = \frac{|M_{n,m,s,-s}(\vec{Q})|^2}{\hbar\omega - E_{n,s}^{\mathrm{ex}}(\vec{Q}) + i\gamma_{\mathrm{ex}} - \Sigma_{n,T}^{\mathrm{ex}}(\vec{Q},\omega)|_{\mathrm{ph}} - \sum_{m'\neq m,s'}\Sigma_{n,m',s,s'}^{\mathrm{ex}}(\vec{Q},\omega)|_{\mathrm{tr}}}. \tag{13}$$

As before, the spin or valley index s on the right-hand side in Eqs. (12) and (13) stands for any one of the two values for which $|g_s| \neq 0$.

For simulations, we consider an electron-doped monolayer of 2D MoSe$_2$ inside an optical microcavity, as shown

in Fig. 1(b). In monolayer MoSe$_2$, the spin splitting of the conduction bands is large ($\sim$35 meV [32]), and the lowest conduction band in each of the K and K' valleys is optically coupled to the topmost valence band [33]. We assume $m_e = m_h = 0.7m_o$, which agrees with the recently
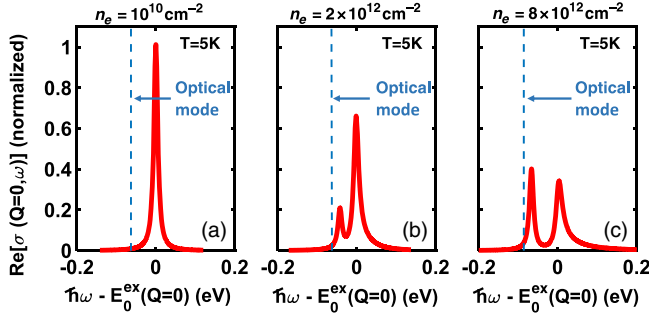
FIG. 2. Calculated real part of the optical conductivity, $\sigma(\vec{Q} = 0, \omega)$, for in-plane (TE) light polarization, is plotted for three different electron densities ($n_e = 10^{10}, 2 \times 10^{12}, 8 \times 10^{12} \text{ cm}^{-2}$) for electron-doped monolayer 2D MoSe$_2$. Only the lowest energy exciton state is considered in the calculations. The spectra are all normalized to the peak optical conductivity value at zero electron density. $T = 5$ K. The frequency axis is offset by the exciton energy $E^{ex}_{n=0,s}(\vec{Q} = 0)$. The position of the cavity optical mode is also indicated (see Fig. 3). Two prominent peaks are seen in the absorption spectra when the electron density exceeds $\sim 10^{12} \text{ cm}^{-2}$. Each peak corresponds to a state that is a superposition of the exciton and trion states [21]. The spectral weight shifts from the higher energy peak to the lower energy peak with the increase in the electron density.

measured value of $0.35m_o$ for the exciton reduced mass [34]. The cavity optical mode has a parabolic dispersion with a photon mass of $10^{-5}m_o$. $|\chi(z = 0)|^2 = 10 \ \mu\text{m}^{-1}$. We use a wave-vector-dependent dielectric constant $\epsilon(\vec{q})$, appropriate for 2D materials [21,26], to screen the Coulomb potentials. We assume that $\gamma_{ex} = \gamma_{tr} = \gamma_p \sim 6$ meV [35]. We compute exciton and trion eigenfunctions and eigenenergies for different momenta and electron densities as described by Rana *et al.* [21].

Figure 2 shows the real part of the optical conductivity (optical absorption spectra) for three different electron densities, and Fig. 3 shows the corresponding polariton dispersions (dashed lines) as well as the spectral densities of the photon, the transverse exciton, and the transverse bound trion. We assume in simulations that the cavity optical mode is tuned ~ 20 meV below the lower energy peak in the optical absorption spectra (as indicated in Fig. 2). At the lowest electron density ($n = 10^{10} \text{ cm}^{-2}$), the lower energy peak in the optical absorption spectrum has essentially no optical oscillator strength and all the spectral weight lies in the higher energy peak [which is the only one seen in Fig. 2(a)]. The higher and lower energy states at such small electron densities correspond to essentially pure exciton and pure (bound) trion states, respectively [21]. The resulting polariton dispersion shows two bands, UP (upper polariton) and LP (lower polariton), which represent exciton polaritons [Figs. 3(a) and (b)]. The bound trion states do not form polaritons as they have no oscillator strength. When the electron density increases beyond $\sim 10^{12} \text{ cm}^{-2}$, the exciton and trion states become coupled
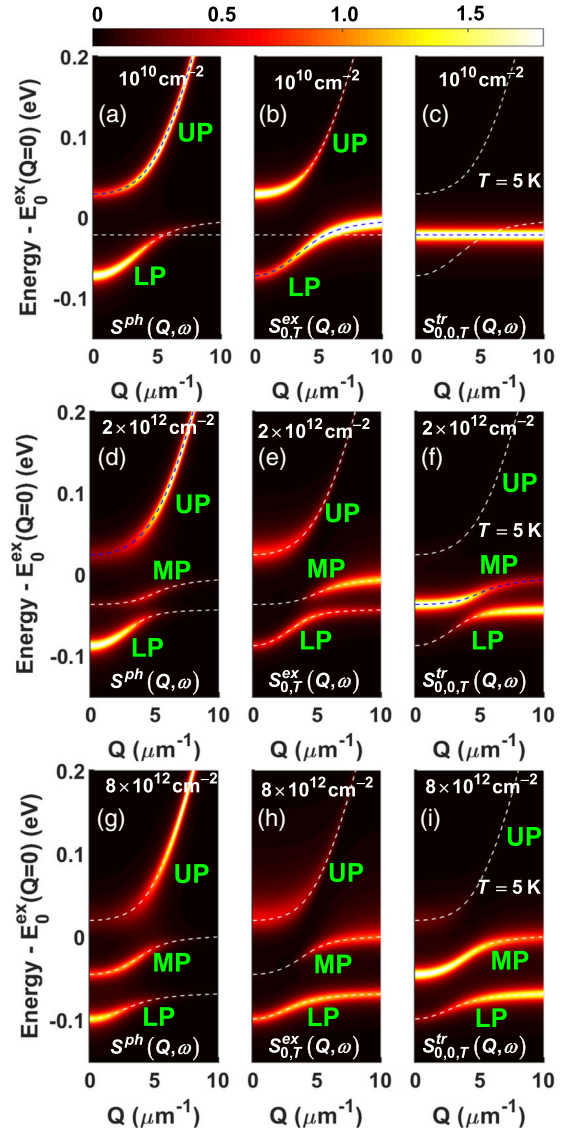

FIG. 3. Calculated exciton-trion polariton (ETP) energy dispersions (dashed lines) and the spectral densities of the photon [$S^{ph}(\vec{Q}, \omega)$], the transverse exciton [$S^{ex}_{n=0,T}(\vec{Q}, \omega)$], and the transverse bound trion [$S^{tr}_{n=0,m=0,T}(\vec{Q}, \omega)$], are plotted for three different electron densities ($n_e = 10^{10}, 2 \times 10^{12}, 8 \times 10^{12} \text{ cm}^{-2}$) for an electron-doped monolayer 2D MoSe$_2$ inside an optical cavity [Fig. 1(b)]. In each case, the cavity optical mode is tuned ~ 20 meV below the lower energy peak in the optical absorption spectra (as indicated in Fig. 2). $T = 5$ K. The unit in the color bar is 10^{-13} s.

as a result of strong Coulomb interactions, and the resulting optical absorption spectra show two prominent peaks [Fig. 2(b)]. Each peak corresponds to a state that is a superposition of 2-body exciton and 4-body (bound) trion states [21]. The polariton dispersion for $n = 2 \times 10^{12} \text{ cm}^{-2}$ shows three bands: UP, MP (middle polariton), and LP [Figs. 3(d)–(f)]. The Rabi splitting between the LP and MP bands is, however, small and reflects the fact that the lower energy peak in the optical absorption spectra [Fig. 2(b)]

does not have much optical oscillator strength. As the electron density increases further, the spectral weight continues to shift from the higher energy peak in the absorption spectrum to the lower energy peak and, in addition, the higher energy peak broadens, becomes non-Lorentzian, and develops a pedestal as a result of exciton-electron scattering (i.e., Coulomb coupling of the exciton and unbound trion states). This pedestal is visible on the higher energy side of the peak in Fig. 2(c) for $n = 8 \times 10^{12}$ cm^{-2}. When $n = 8 \times 10^{12}$ cm^{-2}, the increase in the oscillator strength of the lower energy peak is reflected in the large Rabi splitting between the LP and MP polariton bands in Figs. 3(g)–(i). Also visible in Figs. 3(g)–(i) is the extremely large broadening of the UP band from dephasing caused by exciton-electron scattering at this large doping density. The spectral densities obey the following sum rule:

$$\int \frac{d\omega}{2\pi} [S^{\mathrm{ph}}(\vec{Q}, \omega) + S^{\mathrm{ex}}_{n=0,T}(\vec{Q}, \omega) + S^{\mathrm{tr}}_{n=0,m=0,T}(\vec{Q}, \omega)] = 3. \quad (14)$$

The results presented in this Letter highlight the important role played by the Coulomb interaction between trions and excitons in coupling trions and photons to enable ETPs. Since this Coulomb interaction depends on the doping density, the spectral weights and the energies of ETP bands can be modified in a significant way by varying the doping density, as shown in Fig. 3. The electron density in 2D TMD materials can be varied from zero to mid-10^{13} cm^{-2} by electrostatic gating, thereby opening up opportunities for novel electrically controlled polariton devices. The 4-body trion component of ETPs contains a tightly bound charged 3-body complex surrounded by a Fermi hole (Fig. 1). This Fermi hole is not too different from the exchange hole that surrounds every electron in an electron-doped semiconductor [36,37]. One can therefore expect ETPs to move in response to electrochemical potential gradients by virtue of their trion component, thereby enabling electrical control over polariton dynamics. Electrical and optical transport experiments performed on exciton-trion superposition states in semiconductor quantum wells support this conjecture [38]. In exciton-polaritons, polariton-polariton interactions and polariton relaxation processes, which play an important role in polariton lasers and condensates, are determined by their exciton component [39,40]. In ETPs, exciton and trion components will determine polariton interactions. Experimental efforts geared toward understanding these interactions have been recently reported [2,41]. An accurate description of the structure and composition of ETPs, as attempted in this Letter, will be critical in understanding and modeling these interactions. The direct Coulomb interactions between excitons are weak due to their charge-neutral nature, and

short-range exchange interactions tend to dominate [39]. In contrast, the direct Coulomb coupling between trions, although screened by the Fermi holes, is expected to be stronger and could play an important role in polariton-polariton interactions. These interactions are expected to be also strongly affected by phase space filling effects (at large electron or hole densities) and doping depletion effects (at large polariton densities). We expect that the work presented in this Letter will stimulate further exploration of the physics and applications of ETPs in 2D materials.

[1] S. Dhara, C. Chakraborty, K. M. Goodfellow, L. Qiu, T. A. O'Loughlin, G. W. Wicks, S. Bhattacharjee, and A. N. Vamivakas, Nat. Phys. **14**, 130 (2018).

[2] R. P. A. Emmanuele, M. Sich, O. Kyriienko, V. Shahnazaryan, F. Withers, A. Catanzaro, P. M. Walker, F. A. Benimetskiy, M. S. Skolnick1, A. I. Tartakovskii, I. A. Shelykh, and D. N. Krizhanovskii, Nat. Commun. **11**, 3589 (2020).

[3] J. Cuadra, D. G. Baranov, M. Wersall, R. Verre, T. J. Antosiewicz, and T. Shegai, Nano Lett. **18**, 1777 (2018).

[4] S. Dufferwiel, T. P. Lyons, D. D. Solnyshkov, A. A. P. Trichet, F. Withers, S. Schwarz, G. Malpuech, J. M. Smith, K. S. Novoselov, M. S. Skolnick, D. N. Krizhanovskii, and A. I. Tartakovskii, Nat. Photonics **11**, 497 (2017).

[5] M. Sidler, P. Back, O. Cotlet, A. Srivastava, T. Fink, M. Kroner, E. Demler, and A. Imamoglu, Nat. Phys. **13**, 255 (2017).

[6] O. Kyriienko, D. N. Krizhanovskii, and I. A. Shelykh, Phys. Rev. Lett. **125**, 197402 (2020).

[7] M. Combescot and O. Betbeder-Matibet, Solid State Commun. **126**, 687 (2003).

[8] S.-Y. Shiau, M. Combescot, and Y.-C. Chang, Phys. Rev. B **86**, 115210 (2012).

[9] T. C. Berkelbach, M. S. Hybertsen, and D. R. Reichman, Phys. Rev. B **88**, 045318 (2013).

[10] R. A. Sergeev and R. A. Suris, Phys. Solid State **43**, 746 (2001).

[11] E. Courtade, M. Semina, M. Manca, M. M. Glazov, C. Robert, F. Cadiz, G. Wang, T. Taniguchi, K. Watanabe, M. Pierre, W. Escoffier, E. L. Ivchenko, P. Renucci, X. Marie, T. Amand, and B. Urbaszek, Phys. Rev. B **96**, 085302 (2017).

[12] R. Rapaport, E. Cohen, A. Ron, E. Linder, and L. N. Pfeiffer, Phys. Rev. B **63**, 235310 (2001).

[13] V. Shahnazaryan, V. K. Kozin, I. A. Shelykh, I. V. Iorsh, and O. Kyriienko, Phys. Rev. B **102**, 115310 (2020).

[14] See Supplemental Material at http://link.aps.org/supplemental/10.1103/PhysRevLett.126.127402 for a discussion of different theoretical models for trions, and for polaritons involving trions, that have been proposed in the literature and for comparison of these models to the work presented here, which includes Refs. [15–20].

[15] A. Esser, R. Zimmermann, and E. Runge, Phys. Status Solidi (b) **227**, 317 (2001).

[16] M. Combescot, O. Betbeder-Matibet, and F. Dubin, Eur. Phys. J. B **42**, 63 (2004).

[17] M. Combescot and S.-Y. Shiau, *Excitons and Cooper Pairs* (Oxford University Press, Oxford, UK, 2016).

[18] G. Plechinger, P. Nagler, A. Arora, R. Schmidt, A. Chernikov, A. G. del Aguila, P. C. M. Christianen, R. Bratschitsch, C. Schuller, and T. Korn, Nat. Commun. **7**, 12715 (2016).

[19] R. Schmidt, M. Knap, D. A Ivanov, J.-S. You, M. Cetina, and E. Demler, Rep. Prog. Phys. **81**, 024401 (2018).

[20] F. Chevy, Phys. Rev. A **74**, 063628 (2006).

[21] F. Rana, O. Koksal, and C. Manolatou, Phys. Rev. B **102**, 085304 (2020).

[22] F. Rana, O. Koksal, M. Jung, G. Shvets, and C. Manolatou, Phys. Rev. B **103**, 035424 (2021).

[23] D. K. Efimkin and A. H. MacDonald, Phys. Rev. B **95**, 035417 (2017).

[24] R. A. Suris, in *Optical Properties of 20 Systems with Interacting Electrons*, edited by W. Ossau and R. Suris, NATO Science Series (Kluwer Academic Publishers, Boston, 2003), pp. 111–124.

[25] Y. W. Chang and D. R. Reichman, Phys. Rev. B **99**, 125421 (2019).

[26] C. Zhang, H. Wang, W. Chan, C. Manolatou, and F. Rana, Phys. Rev. B **89**, 205436 (2014).

[27] D. Xiao, G.-B. Liu, W. Feng, X. Xu, and W. Yao, Phys. Rev. Lett. **108**, 196802 (2012).

[28] C. Manolatou, H. Wang, W. Chan, S. Tiwari, and F. Rana, Phys. Rev. B **93**, 155422 (2016).

[29] H. Wang, C. Zhang, W. Chan, C. Manolatou, S. Tiwari, and F. Rana, Phys. Rev. B **93**, 045407 (2016).

[30] H. Haug and S. W. Koch, *Quantum Theory of the Optical and Electronic Properties of Semiconductors* (World Scientific Publishing, Singapore, 1990).

[31] J. J. Hopfield, Phys. Rev. **112**, 1555 (1958).

[32] K. Kosmider, J. W. Gonzalez, and J. Fernandez-Rossier, Phys. Rev. B **88**, 245436 (2013).

[33] G.-B. Liu, W.-Y. Shan, Y. Yao, W. Yao, and D. Xiao, Phys. Rev. B **88**, 085433 (2013).

[34] M. Goryca, J. Li, A. V. Stier, T. Taniguchi, K. Watanabe, E. Courtade, S. Shree, C. Robert, B. Urbaszek, X. Marie, and S. A. Crooker, Nat. Commun. **10**, 4172 (2019).

[35] M. Selig, G. Berghuser, A. Raja, P. Nagler, C. Schuller, T. F. Heinz, T. Korn, A. Chernikov, E. Malic, and A. Knorr, Nat. Commun. **7**, 13279 (2016).

[36] H. Haug and S. W. Koch, *Quantum Theory of the Optical and Electronic Properties of Semiconductors* (World Scientific Publishing, Singapore, 1990).

[37] G. D. Mahan, in *Many-Particle Physics* (Plenum Publishers, New York, USA, 2000), Chap. 5.

[38] D. Sanvitto, F. Pulizzi, A. J. Shields, P. C. M. Christianen, S. N. Holmes, M. Y. Simmons, D. A. Ritchie, J. C. Maan, and M. Pepper, Science **294**, 837 (2001).

[39] H. Deng, H. Haug, and Y. Yamamoto, Rev. Mod. Phys. **82**, 1489 (2010).

[40] C. Schneider, A. Rahimi-Iman, N. Y. Kim, J. Fischer, I. G. Savenko, M. Amthor, M. Lermer, A. Wolf, L. Worschech, V. D. Kulakovskii, I. A. Shelykh, M. Kamp, S. Reitzenstein, A. Forchel, Y. Yamamoto, and S. Hfling, Nature (London) **497**, 348 (2013).

[41] L. B. Tan, O. Cotlet, A. Bergschneider, R. Schmidt, P. Back, Y. Shimazaki, M. Kroner, and A. Imamoglu, Phys. Rev. X **10**, 021011 (2020).